

# Robust M-estimation for Partially Observed Functional Data

Yeonjoo Park,

Management Science and Statistics, University of Texas at San Antonio

Xiaohui Chen, and Douglas G. Simpson \*

Department of Statistics, University of Illinois at Urbana-Champaign

## Abstract

Irregular functional data in which densely sampled curves are observed over different ranges pose a challenge for modeling and inference, and sensitivity to outlier curves is a concern in many applications. This paper investigates a class of robust M-estimators for partially observed functional data modeling irregular structure using a missing data framework. We derive asymptotic normality of functional M-estimator under the proposed framework and show root- $n$  rates of convergence. Furthermore, we propose a class of functional trend tests to find significant directions in the trend of location. For the implementation of the inferential test, we adopt a joint bootstrap approach. The performance is demonstrated in simulations and application to data from quantitative ultrasound analysis.

*Keywords:* Bootstrap; Functional central limit theorem; Irregular functional data; Trend inference

---

\*X. Chen's research is supported in part by NSF CAREER Award DMS-1752614 and UIUC Research Board Award RB18099. D. G. Simpson's research is supported in part by NIH Grant R01HD089935.

# 1 Introduction

With advances in instrumentation and the capability to acquire data densely over a continuum, function-valued data acquisition is increasingly common in many fields; see, e.g. [Ramsay & Silverman \(2005\)](#) and [Horváth & Kokoszka \(2012\)](#). Earlier works on functional data focused in large part on regular functional data, where the functional samples are densely collected over a common domain, or sparse functional data, in which the functional response for each subject is sparsely sampled with a small number of irregularly spaced measurements over the domain. In recent years, however, applications have emerged that produce partially observed functional data, where different curves are densely observed over different ranges. Several recent works have begun addressing the analysis of partially observed functional data, notably, estimation of the unobserved part of curves ([Kraus \(2015\)](#); [Kneip & Liebl \(2019\)](#)), prediction ([Liebl \(2013\)](#); [Goldberg et al. \(2014\)](#); [Delaigle & Hall \(2016\)](#)), classification ([Delaigle & Hall \(2013\)](#); [Stefanucci et al. \(2018\)](#); [Mojirsheibani & Shaw \(2018\)](#); [Kraus & Stefanucci \(2018\)](#); [Park & Simpson \(2019\)](#)), functional regression ([Gellar et al. \(2014\)](#)), and inferences ([Gromenko et al. \(2017\)](#); [Kraus \(2019\)](#)).

Robustness to atypical curves or deviations from Gaussian variation is a concern in modeling and inference, especially for partially observed data. [Park & Simpson \(2019\)](#) demonstrated that t-type heavy-tailed models for functional data had a superior predictive performance for probabilistic classification of quantitative ultrasound (QUS) measurements, which extract diagnostic information on biological tissues, such as tumors, from the ultrasound radio frequency backscattering signals. Here the backscattered spectrum is captured by transducer by scanning the region of interest and an attenuation adjusted backscatter coefficient (BSC), which forms the functional curve spanning the frequency range of the transducer, is calculated. [Wirtzfeld et al. \(2015\)](#) presented data from an inter-laboratory diagnostic ultrasound study in which two types of induced mammary tumors were scanned using multiple transducers of varying center frequencies: 4T1 tumors in mice and MAT tumors in rats. Figure 1 shows a subset of the data produced. The resulting BSC curves are observed over varying frequency ranges depending on transducers used in scanning, and

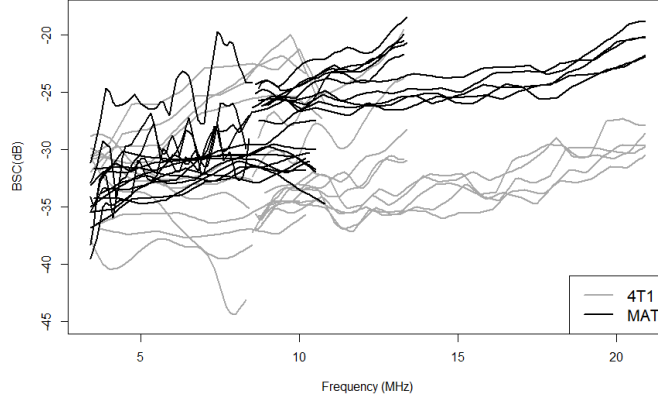


Figure 1: BSC data example by scanning two mammary tumors, 4T1 and MAT.

at the same time, several curves show atypical behaviors, especially at the lower frequency ranges in the 4T1 group.

We model these curves as partially observed functional data and develop robust methods for estimation and inference that address the extra-Gaussian variation in the curves. The example motivates us to study two main topics in this article: (i) propose a robust functional data analysis tool to estimate the location parameter, which can be applied to partially observed functional data, and (ii) develop an inferential tool based on the derivation of asymptotic properties of the proposed robust estimator.

Several authors have studied robust estimation for fully observed functional data, see [Fraiman & Muniz \(2001\)](#), [Cuevas et al. \(2007\)](#), and [López-Pintado & Romo \(2009, 2011\)](#). They extended the data-depth notion in robust multivariate data analysis to functional data and defined depth weighted robust estimators. In another direction, [Locantore et al. \(1999\)](#), [Gervini \(2008\)](#) and [Sinova et al. \(2018\)](#) developed robust estimators from fully functional approach with investigations on robustness and asymptotic properties of the estimators. However, none of these robust methods for complete functional data are directly applicable to partially observed functional data.

We propose a new class of functional M-estimator by extending a class of M-estimators [Huber \(2005\)](#) to functional data. The approach considered here is in contrast to the recent functional location M-estimators developed in [Sinova et al. \(2018\)](#), which imposed a

bounded M-estimator score function on the norm of the entire functional deviation from the location parameter function. Our approach builds the functional M-estimator in a cross-sectional manner to take advantage of all available curve data while adapting to uneven patches in the response samples due to partial observation of individual curves. The difference will be presented in detail in Section 2.2. Even with fully observed functional data, the cross-sectional approach considered here potentially handles outlying patches in different spatial locations better than the approach of applying a robust pseudo-norm to the entire function.

We employ a missing data formulation to deal with the partially observed functional data. This type of framework was previously considered by Kraus (2015, 2019) and Park (2017) in consideration of functional mean and covariance estimation. Here we generalize the conditions on the partial information filtering. Based on this framework, we study asymptotic properties of the proposed estimator including the consistency and asymptotic Gaussian process approximations. Furthermore, we adapt the results to develop robust functional trend tests with bootstrap inferences. The robustness of the M-estimators is investigated by influence analysis and the bounded effect of outlying curves is shown in the estimation of a functional location parameter. Simulation studies and analysis of data from a quantitative ultrasound study (QUS) demonstrate the properties of the methods.

Section 2 defines the new class of functional M-estimators and the approach taken here has the advantage of being implementable for partially observed functional data with bounded influence function. Section 3 establishes the theoretical properties of M-estimator including the consistency and the Gaussian process approximations of the estimates. Also, the application of Gaussian approximation to the functional trend test is presented with the bootstrap inferences for practical implementation. The remaining sections include simulations and real data example.

## 2 M-estimator for Partially Observed Functional Data

### 2.1 Modeling assumptions

Let  $X_1(t), X_2(t), \dots, X_n(t)$  be functional samples observed over varying subsets,  $S_1, S_2, \dots, S_n$ , of a compact set  $C$ . Similar to [Kraus \(2015, 2019\)](#) and [Park \(2017\)](#), we consider the observed curves to be the result of filtering latent full information curves  $Y_1(t), Y_2(t), \dots, Y_n(t)$  on  $C$  by independent indicator processes  $\delta_1(t), \delta_2(t), \dots, \delta_n(t)$ , where

$$\delta_i(t) = \begin{cases} 1, & \text{if } Y_i(t) \text{ is observed;} \\ 0, & \text{if } Y_i(t) \text{ is unobserved;} \end{cases}$$

for  $t \in C$  and  $i = 1, \dots, n$ . We make general assumptions about the nature of the filtering functions  $\delta_i$  and the modeling assumptions include the following:

M1: The stochastic processes,  $(Y_i, \delta_i) := \{(Y_i(t), \delta_i(t)), t \in C\}$ ,  $i = 1, \dots, n$  are independent and identically distributed on  $(\Omega, \mathcal{F}, \mathbb{P})$  and jointly  $\mathcal{F}$ -measurable.

M2:  $\delta_i := \{\delta_i(t) : t \in C\}$ ,  $i = 1, \dots, n$  are i.i.d. marginal Bernoulli processes defined as indicator functions for sets  $S_i$ , such that the covariance function  $c(s, t) = \text{Cov}(\delta_1(s), \delta_1(t))$  is twice continuously differentiable and for any  $s, t \in C$ ,

$$K_1 \leq c_{st}(s, t) \leq K_2 \tag{1}$$

for some constants  $K_1, K_2 > 0$ , where  $c_{st}(s, t) = \frac{\partial^2}{\partial s \partial t} c(s, t)$  is the mixed second partial derivative.

M3:  $E(\delta_i(t)) = b(t)$ ,  $t \in C$ , where  $b(\cdot)$  is uniformly continuous and bounded away from zero,  $\inf_{t \in C} b(t) > 0$ .

M4:  $Y_i(t)$  and  $\delta_i(t)$  are independent for  $i = 1, \dots, n$ .

As seen in Condition M1, the use of robust estimator avoids the need for restrictive moment assumptions on the process  $Y_i$ , and the proposed approach will enable the analysis of partially observed processes from heavy-tailed or outlier-prone sampling distributions.

In Condition M2, (1) requires that the mixed second partial derivative of  $c(s, t)$  is uniformly bounded below and above. This condition implies that the natural distance  $d(s, t) = \sqrt{c(s, s) + c(t, t) - 2c(s, t)}$  induced by the covariance function  $c(s, t)$  of the indicator process is equivalent to the Euclidean distance  $|s - t|$  in the sense that the covering numbers of index set  $C$  under the two metrics are on the same order. Indeed, by Taylor's expansion for  $t = s + \varepsilon$  and the symmetry (i.e.,  $c_s = c_t$  and  $c_{st} = c_{ts}$ ), we can compute as  $\varepsilon \rightarrow 0$ ,

$$\begin{aligned} c(s, s + \varepsilon) &= c(s, s) + \varepsilon c_t(s, s) + \frac{\varepsilon^2}{2} c_{tt}(s, s) + o(\varepsilon^2), \\ c(s + \varepsilon, s + \varepsilon) &= c(s, s) + \varepsilon [c_s(s, s) + c_t(s, s)] + \frac{\varepsilon^2}{2} [c_{ss}(s, s) + 2c_{ts}(s, s) + c_{tt}(s, s)] + o(\varepsilon^2), \end{aligned}$$

which imply that

$$d(s, s + \varepsilon)^2 = \varepsilon^2 c_{ts}(s, s) + o(\varepsilon^2).$$

Then it follows from (1) that the covariance metric (in terms of curvature) is equivalent to the Euclidean metric on the index set  $C$ . For example, a random interval  $S_i = [l_i, u_i] \subset C$ , where  $l_i = \min(v_{i1}, v_{i2})$  and  $u_i = \max(v_{i1}, v_{i2})$  with  $v_{ij}$ ,  $j = 1, 2$ , i.i.d. from random variable  $V$  with the support of  $C$  satisfies the Condition M2. If the support of  $V$  is wider than  $C$ , we can modify  $S_i$  by truncating lower and upper bounds,  $l_i$  and  $u_i$ , with the lower and upper bounds of  $C$ . Condition M2 is needed for proving the uniform convergence of the average of sample indicator processes  $\delta_i(t)$ ,  $i = 1, \dots, n$ , to  $b(t)$ . Kraus (2019) specified such sup-norm convergence of the averaged sample indicator processes as one of conditions. Here we only impose mild explicit condition on the regularity of the covariance functions to derive large sample properties of the proposed robust estimator that we shall see in Section 3.

Condition M3 implies that the full range is covered by a sufficient portion of the data for sufficiently large sample sizes. For the previous example of the random interval  $S_i = [l_i, u_i]$ , the support of  $V$  should have positive probabilities at both boundaries of  $C$  to ensure the positive  $b(t)$  is bounded away from zero. Lastly, letting  $P$  denote the joint probability measure for  $(Y, \delta)$ , Condition M4 implies that  $P = P_Y \cdot P_\delta$ , where  $P_Y$  and  $P_\delta$  denote the marginal probability measures for  $Y$  and  $\delta$  on  $C$ , respectively. Along with Condition M3,

it enables the estimation of the functional parameter of  $Y$  based on the partially observed functions  $X$ .

## 2.2 Marginal M-estimator

For partially observed samples  $X_1(t), \dots, X_n(t)$ , we define the functional M-estimator  $\hat{\theta}_n(t)$  under the cross-sectional approach by minimizing the criterion marginally for all values of  $t$  in parallel as below,

$$\hat{\theta}_n(t) = \operatorname{argmin}_{h \in \mathbb{R}} \sum_{i=1}^n \delta_i(t) \rho(X_i(t) - h), \quad (2)$$

for  $t \in \mathcal{C}$  satisfying  $\sum_{i=1}^n \delta_i(t) > 0$ , where  $\rho(\cdot)$  is a real-valued loss function. Otherwise, the estimator is undefined. In other words, for fixed  $t$ ,  $\hat{\theta}_n(t)$  represents a pointwise M-estimator calculated based on the information observed at grid  $t$ . If we observe undefined  $\hat{\theta}_n(t)$  at certain range in  $\mathcal{C}$  under finite sample size, it can be estimated through interpolation or smoothing methods when smoothness and continuity of  $\hat{\theta}_n(t)$  is assumed. In practice, discretized partial curves are observed on fine grids and interpolation can be applied for the estimation. For example, if  $\rho(x) = x^2$  then  $\hat{\theta}_n(t)$  reduces to the weighted sample mean function,

$$\bar{X}_\delta(t) = \frac{\sum_{i=1}^n \delta_i(t) X_i(t)}{\sum_{i=1}^n \delta_i(t)}, \quad t \in \mathcal{C},$$

and [Kraus \(2019\)](#) observed the consistency of  $\bar{X}_\delta$  for estimating the mean function of  $Y$  if  $Y$  and  $\delta$  are independent. Now we consider the general class of marginal M-estimators with general  $\rho$ , motivated by the need for robust alternatives to the weighted sample mean. The following conditions are assumed for the loss function  $\rho$ .

- A1  $\rho : \mathbb{R} \rightarrow \mathbb{R}$  is continuous even function and strictly increasing on  $\mathbb{R}^+$  with  $\rho(0) = 0$ .
- A2  $\rho$  increases at most linearity in the tails;  $|\rho(x_1) - \rho(x_2)| \leq L|x_1 - x_2|$  for some constant  $L$ .
- A3  $\rho$  is differentiable and  $\psi = \rho'$  is continuous.

A4  $\dot{\psi} = \psi'$  is almost everywhere differentiable and Lipschitz continuous;  $|\dot{\psi}(x_1) - \dot{\psi}(x_2)| \leq K|x_1 - x_2|$  for some constant  $K$ .

Note that Condition A2-A3 imply the bounded  $\psi$  and it enables handling heavy-tailed behavior of  $Y$  without assuming moment conditions on it. The asymptotic normality of functional M-estimator will be demonstrated based on Condition A4 in Section 3.3.

Under given conditions of  $\rho$ , functional M-estimator marginally solves the estimating equation,

$$\frac{1}{n} \sum_{i=1}^n \delta_i(t) \psi(X_i(t) - \hat{\theta}_n(t)) = 0, \quad t \in C. \quad (3)$$

The proposed M-estimator is defined as a marginal minimizer over  $t \in C$  under a cross-sectional approach. On the other hand, a class of M-estimators of the functional location proposed by Sinova et al. (2018) minimizes functional norm in Hilbert space over  $C$  with the form

$$\hat{\theta}_n^{\mathbb{H}}(\cdot) = \operatorname{argmin}_{h \in \mathbb{H}} \frac{1}{n} \sum_{i=1}^n \rho(\|Y_i(\cdot) - h(\cdot)\|_{\mathbb{H}}),$$

where  $\|\cdot\|_{\mathbb{H}}$  is a norm for Hilbert space  $\mathbb{H}$ . They established the consistency of the estimator and derived the influence functions to investigate its robustness. However, the estimator  $\hat{\theta}_n^{\mathbb{H}}$  is not directly applicable to the partially observed functional data. Also, it may not be able to capture local information by estimating the location parameter based on the norm of the whole curve over  $C$ . Meanwhile, the proposed M-estimator is applicable to general functional data and it turns out to provide consistent estimates of functional location parameter under regularity conditions as we will see in Section 3. Even under the complete functional data of  $\delta_i(t) = 1, i = 1, \dots, n, t \in C$ , the proposed marginal approach offers an alternative wherein the robustness or outlier resistance of the estimator is controlled locally along with the function rather than on the overall norm of the function. We will see the advantage of the marginal approach in simulation studies of Section 5.



## 2.3 Estimability and identifiability

In this section, we define the functional M-location parameter, a theoretical version of  $\hat{\theta}_n(t)$ , and investigate its properties. Based on the joint probability measure  $P$  for  $(Y, \delta)$ , functional M-location parameter  $\theta(t)$  is defined as,

$$\theta(t) = \operatorname{argmin}_{h \in \mathbb{R}} E_P[\delta(t)\rho(Y(t) - h)], \quad t \in C. \quad (4)$$

Under Conditions A1-A3,  $\theta(t)$  also marginally satisfies

$$E_P[\delta(t)\psi(Y(t) - \theta(t))] = 0, \quad t \in C. \quad (5)$$

We first investigate the property of functional M-location parameter under symmetric  $Y$  with the following proposition. Let  $\Theta$  represent a functional parameter set in Reimann integrable  $L^2(C)$  space, which includes piecewise continuous functions with a finite number of bounded jumps.

**Proposition 2.1** (Symmetric marginal distributions). *Under conditions of M1, M4, A1-A3, if the marginal density of  $Y(t)$  for each  $t \in C$  is symmetric about a deterministic function  $\alpha(t) \in \Theta$ , i.e.,  $Y(t) - \alpha(t)$  and  $\alpha(t) - Y(t)$  have the same distribution,  $\theta(t) = \alpha(t)$ .*

Proposition 2.1 implies that  $\theta(t)$  represents the functional center when the marginal density of  $Y(t)$  is symmetric for each  $t \in C$ . In the absence of symmetry, the following condition enables us to define the functional parameter being estimated up to an additive constant that depends only on the marginal distribution.

B1 [Transformable strong stationarity] There exists a deterministic function  $\alpha(t) \in \Theta$ , such that, for  $Z(t) = Y(t) - \alpha(t)$ ,  $F_Z(z_{t_1+\tau}, \dots, z_{t_n+\tau}) = F_Z(z_{t_1}, \dots, z_{t_n})$ , for all  $\tau, t_1, \dots, t_n \in \mathbb{R}$  and for all  $n \in \mathbb{N}$ , where  $F_Z(z_{t_1}, \dots, z_{t_n})$  denotes the cumulative distribution function of joint distribution. Thus,  $F_Z(z_{t_k}) \equiv F_Z(z_{t_1}) \equiv F_Z(z)$  for all  $k \in \mathbb{N}$ .

We then derive the following proposition under generalized distribution of  $Y$ .

**Proposition 2.2** (Identifiable location function). *Under conditions of M1, M4, A1-A3, B1, with the translation function  $\alpha(t)$ ,  $\theta(t) = \alpha(t) + c$ , where a constant  $c$  is determined by  $F_Z$ .*

It implies that  $\theta(t)$  is a well-defined location function parameter that can inherit any smoothness or bounded jumps up to an additive constant depending on  $\alpha(t)$ .

For the investigation on asymptotic relation between  $\hat{\theta}_n(t)$  and  $\theta(t)$ , we now define the weighted M functional,

$$M(t, h, P) = E_P[\delta(t)\{\rho(Y(t) - h(t)) - \rho(Y(t))\}], \quad (6)$$

and  $\theta(t)$  equivalently marginally minimizes  $M(t, h, P)$  for  $t \in C$ ; cf. Section 3.2 of [Huber \(2005\)](#) for the univariate case. Under Conditions A1-A2, the expectation in (6) exists for every probability measure  $P$  and we assume the following general conditions:

D1  $\sup_{\theta \in \Theta} \sup_{t \in C} |M(t, \theta, P_n) - M(t, \theta, P)| \xrightarrow{P} 0$ , where  $P_n$  denotes a sequence of measures converges weakly to a measure  $P$ .

D2 For every  $\epsilon > 0$ ,  $\inf_{\theta^* \in \Theta} \inf_{t \in C} \{M(t, \theta^*, P) - M(t, \theta, P) : |\theta^*(t) - \theta(t)| > \epsilon\} > 0$ .

Condition D1 requires the uniform convergence of weighted M-functional over the parameter space  $\theta \in \Theta$  and  $t \in C$ . As an example, if  $P_n$  denotes the empirical measure of  $\{Y_i(t), \delta_i(t), t \in C\}_{i=1}^n$ , then for given  $\theta \in \Theta$ , uniform convergence over  $t \in C$  holds under Condition A2. About the uniform convergence over parameter space, refer to Chapter 5 of [van der Vaart \(2007\)](#) with other possible assumptions to replace uniform convergence over parameter space for the univariate case. Condition D2 implies that, for  $t \in C$ , only  $\theta(t)$  yields a minimum value of  $M(t, h, P)$ , thus it is a well-separated point of minimum at grid  $t$ . It holds under Condition A1 and the derivation of Influence function and the large sample properties will be based on above conditions on functional M.

## 2.4 Robustness and Influence functions

Now we investigate the outlier sensitivity of the estimator measured by the influence function ([Hampel \(1974\)](#)). Here we consider contaminated curve which may show atypical behavior in two manners: atypical behavior in process  $Y$ , for example, with extreme or abnormal values at certain range or along with the whole curve, or outlying behavior in

missing process, such as dependence between  $Y$  and  $\delta$ . In this section, we denote  $\theta(t)$  defined in Section 2.3 by the functional  $T(P)(t)$ . We consider the behavior of  $T$  for arbitrary contamination distributions of the form

$$P_\varepsilon = (1 - \varepsilon)P + \varepsilon\Delta_{(Y^*, \delta^*)} \quad (7)$$

where  $\Delta_{(Y^*, \delta^*)}$  is a point mass distribution concentrated on the functional outlying pair  $(Y^*, \delta^*)$ .

We first establish the continuity of  $T$  uniformly over the contaminating distribution, a robustness property that holds when the score function  $\psi$  is bounded. Note that, by definition,  $P_\varepsilon$  converges weakly to  $P$  as  $\varepsilon \rightarrow 0$ .

**Theorem 2.3** (Contamination Robustness). *Conditions M1, M4, A1-A2, D1-D2 imply*

$$\lim_{\varepsilon \downarrow 0} \sup_{t \in C, (Y^*, \delta^*)} |T(P_\varepsilon)(t) - T(P)(t)| = 0.$$

Next we extend the notion of functional influence function, adapting the definition of Gervini (2008) as

$$IF_T(Y^*, \delta^*)(t) = \lim_{\varepsilon \downarrow 0} \varepsilon^{-1} \{T(P_\varepsilon)(t) - T(P)(t)\}, \quad (8)$$

if the limit exists, where  $P_\varepsilon$  is given in (7). In essence, the influence function is the Gateaux derivative of the functional  $T$  in the direction of contamination  $\Delta_{(Y^*, \delta^*)}$  to the true distribution  $P$ . The corresponding gross-error sensitivity (cf. Gervini (2008)) with the sup-norm metric is given by

$$\gamma_T^\infty = \sup_{t \in C} \{\sup |IF_T(Y^*, \delta^*)(t)| : \text{any } (Y^*, \delta^*)\},$$

we then derive the following Theorem.

**Theorem 2.4** (Influence Robustness). *Under M1, M4, A1-A4, if we assume uniform continuity of the functional  $T(P)(t)$  and  $\inf_{t \in C} |E_P[\delta(t)\dot{\psi}(X(t), \theta(t))]| > 0$  and , then*

$$IF_T(Y^*, \delta^*)(t) = \frac{\delta^*(t)\psi(Y^*(t), \theta(t))}{-E_P[\delta(t)\dot{\psi}(X(t), \theta(t))]}, \quad t \in C, \quad (9)$$

and the boundedness of  $\psi$  implies  $\gamma_T^\infty < \infty$ .

It implies the bounded effect of heavy-tailed behavior of the process  $Y$  or dependent missing process on the functional M-location parameter.

### 3 Large Sample Approximations

#### 3.1 Consistency

In establishing consistency and asymptotic Gaussian approximations for the class of functional M-estimators, a key step is to develop an entropy bound used to establish sup-norm convergence for the averaged indicator processes  $\delta(t)$ . In particular, we establish the convergence of

$$W_n = \sup_{t \in C} \left| n^{-1} \sum_{i=1}^n [\delta_i(t) - b(t)] \right|, \quad (10)$$

where, marginally for each  $t \in C$ ,  $\delta_i(t) \sim \text{Ber}(b(t))$  are i.i.d., and the functions  $t \mapsto \delta_i(t)$  are sampled from a general class on  $C$  satisfying Condition M2.

**Lemma 3.1.** *Under Condition M2, we have*

$$E[W_n] = O(n^{-1/2}).$$

Based on Lemma 3.1, we can show the following consistency of the M-estimator.

**Theorem 3.2** (Uniform consistency). *Under conditions of M1-M4, A1-A3, B1, D1-D2,  $\hat{\theta}_n(t)$  converges to  $\theta(t)$  uniformly over  $t \in C$ .*

The proposed M-estimator  $\hat{\theta}_n(t)$  converges to the functional M-location parameter  $\theta(t)$  uniformly over  $t$ . As stated in Section 2.3, Condition D1 holds under Condition A2.

#### 3.2 Functional Central Limit Theorem

We first derive a general functional central limit theorem for functional sample mean under the missing data framework, previously studied by Park (2017) and Kraus (2019), then adapt the result to obtain an asymptotic Gaussian process approximation for the proposed

M-estimators. Let  $C$  be a compact subset in a general metric space equipped with a metric  $d$  and  $V(t)$ ,  $t \in C$ , be a mean-square continuous process defined on a probability space  $(\Omega, \mathcal{F}, P)$ . We suppose that  $V(t, \cdot)$  is measurable for each  $t \in C$ , and  $V(\cdot, \omega)$  is continuous for each  $\omega \in \Omega$ . We consider the second-order stationary process  $V$  with mean zero and the covariance function  $\gamma$  (i.e.,  $\gamma(s, t) = \text{Cov}(V(s), V(t))$ ,  $s, t \in C$ ), denoted by  $V \sim \text{SP}(0, \gamma)$ . We define the process  $Z_n(t)$  as,

$$Z_n(t) = \frac{\sqrt{n} \sum_{i=1}^n \delta_i(t) V_i(t)}{\sum_{j=1}^n \delta_j(t)}, \quad t \in C.$$

The following result is adapted from a functional central limit theorem of Kraus (2019), here incorporating more general filtering functions  $\delta_i$  as indicated in Condition M2.

**Theorem 3.3** (Functional Central Limit Theorem for partially observed data). *Let  $V_1, \dots, V_n$  be i.i.d. samples of the second-order stationary process  $V$ . Under M2-M4 with replacement of  $Y$  by  $V$ , we have*

$$Z_n \rightsquigarrow GP(0, \vartheta),$$

where  $\vartheta(s, t) = \gamma(s, t) \frac{v(s, t)}{b(s)b(t)}$ ,  $s, t \in C$  and  $v(s, t) = E_{P_\delta}[\delta(s)\delta(t)]$ .

Kraus (2019) specified sup-norm convergence of the averaged sample indicator processes in (10) as one of conditions, here we establish this convergence through Lemma 3.1 under more primitive and explicit Condition M2.

### 3.3 Gaussian Process Approximation of M-Estimator

Building on the uniform consistency of the marginal M-estimators and the functional central limit theorem, the results of this section establish that robust M-Estimators have Gaussian process large sample approximations under weaker conditions than the functional sample mean. In particular, functional M-estimators with bounded score functions automatically satisfy the moment conditions of the functional central limit theorem, without imposing moment conditions on the underlying distribution. For notational simplicity, we denote  $\psi(x - \theta)$  by  $\psi(x, \theta)$ .

**Theorem 3.4** (Asymptotic normality of M-estimator). *Under conditions M1-M4, A1-A4, B1, D1-D2, and if  $E_{P_Y}[\dot{\psi}(Y(t), \theta(t))]$  exists and non-singular almost everywhere on  $\mathcal{C}$ ,*

$$\sqrt{n}(\hat{\theta}_n(t) - \theta(t)) \rightsquigarrow GP(0, \xi),$$

$\xi(s, t) = \varphi(s, t)E_{P_Y}[\dot{\psi}(Y(s), \theta(s))]^{-1}E_{P_Y}[\dot{\psi}(Y(t), \theta(t))]^{-1}$ , where  $\varphi(s, t) = \text{Cov} \{ \psi(Y(t), \theta(t)), \psi(Y(s), \theta(s)) \} \frac{v(s, t)}{b(s)b(t)}$  with  $v(s, t) = E_{P_\delta}[\delta(s)\delta(t)]$ .

### 3.4 Functional Trend Test

Based on Gaussian approximation, we propose a tool for an inference on functional trend. To do this we first show the asymptotic normality of the projection coefficient of the M-estimator.

**Corollary 3.5.** *Under the same conditions of Theorem 3.4, let  $c = \langle \theta(\cdot), \phi(\cdot) \rangle$ , where  $\phi(\cdot)$  is a fixed Riemann integrable  $L^2$  function on  $\mathcal{C}$  and  $\langle \cdot, \cdot \rangle$  represents inner product of fixed functions over  $\mathcal{C}$ ,  $\langle f, g \rangle = \int_{\mathcal{C}} f(t)g(t)dt$ . Let  $\xi(s, t)$  denote the asymptotic covariance function of the functional M-estimator derived in Theorem 3.4 and assume that  $\text{tr}(\xi) < \infty$ . Define  $\zeta_n = \sqrt{n}(\langle \hat{\theta}_n(\cdot), \phi(\cdot) \rangle - c)$ . Then*

$$\zeta_n \rightsquigarrow N(0, \tau^2),$$

where  $\tau^2 = \sum_{r=1}^k \lambda_r \int_{\mathcal{C}} \phi(s)\phi(t)e_r(t)e_r(t)dsdt$ . Here,  $\lambda_r$  and  $e_r(\cdot)$ ,  $r = 1, \dots, k$ , are non-zero eigenvalues and corresponding eigenfunctions of  $\xi$ .  $k$  can be infinity.

Asymptotic confidence intervals derived in Corollary 3.5 can provide valuable information whether or not a trend of interest is significant. In general, we could obtain visual information of functional trend from smoothing technique but statistical inference on such trend enables to detect significant trend in the location parameter. In order to use this result in practice, it is necessary to estimate the relevant eigenvalues. Alternatively, the asymptotic approximation justifies using a bootstrap approach for the assessing statistical significance and this approach is presented in the next section. Examples of application are illustrated in Section 5 and Section 6.

## 4 Bootstrap Inference

In practice, it is challenging to estimate the covariance function structure from partially observed data. It implies the difficulty of the direct use of the derived expression in Corollary 3.5 to estimate asymptotic variance. Accordingly, we propose a bootstrap approach to perform the trend test and name it as a linked bootstrap that jointly resamples  $Y$  and  $\delta$  processes, simultaneously. Under the assumption of missing completely at random in Condition M4, it is ideal to generate partially observed pseudo samples by resampling  $Y$  and  $\delta$  over  $C$ , separately. However, in practice, it is infeasible due to lack of information on unobserved segments of  $X_i(t)$ ,  $i = 1, \dots, n$ . We thus propose to generate pseudo-observations by resampling partially observed curves from the data.

Suppose that  $\mathbf{Y}(t) = [Y_1(t), \dots, Y_n(t)]^T$  and  $\boldsymbol{\delta}(t) = [\delta_1(t), \dots, \delta_n(t)]^T$  are  $Y$  and  $\delta$  information. Let  $\mathbf{U} = [\mathbf{U}_1, \dots, \mathbf{U}_n]^T$  denote  $(n \times n)$  matrix, where  $\mathbf{U}_i \sim \text{multinomial}(1, \text{rep}(1/n, n))$ . Here  $\mathbf{U}_i$  tells which functional curve is chosen for the  $i$ th bootstrap sample. Then the bootstrapped functional vector is generated by  $\mathbf{Y}^*(t) = [Y_1^*(t), \dots, Y_n^*(t)]^T = \mathbf{U}\mathbf{Y}(t)$  and  $\boldsymbol{\delta}^*(t) = [\delta_1^*(t), \dots, \delta_n^*(t)]^T = \mathbf{U}\boldsymbol{\delta}(t)$ . Key idea of joint resampling is the use of the same  $\mathbf{U}_i$  to generate  $Y_i^*$  and  $\delta_i^*$ , which is corresponding  $X_i^*$  eventually, where  $\mathbf{X}^*(t) = [X_1^*(t), \dots, X_n^*(t)]^T = \mathbf{U}\mathbf{X}(t)$ . The following proposition shows that  $Y_i^*$  and  $\delta_i^*$  are asymptotically uncorrelated, which supports the use of bootstrapped samples for the inference on partially observed data.

**Proposition 4.1.** *Suppose that the  $i$ th bootstrap pair is resampled through the linked bootstrap,  $Y_i^*(t) = \mathbf{U}_i^T Y(t)$  and  $\delta_i^*(t) = \mathbf{U}_i^T \delta(t)$ . Then, under M4,  $\text{Cov}(Y_i^*(t), \delta_i^*(t))$  is asymptotically 0 for  $t \in C$ .*

The bootstrap-based inference on functional trend can be described as following steps.

Step 1: Resample pseudo partially observed data  $\{X_i^*(t)\}_{i=1}^n$  with replacement from  $\{X_i(t)\}_{i=1}^n$ .

Step 2: Calculate the M-estimator  $\hat{\theta}_n^*(t)$  from the pseudo-observations  $\{X_i^*(t)\}_{i=1}^n$ .

Step 3: Project  $\hat{\theta}_n^*(t)$  to the direction of interest  $\phi(t)$  and calculate  $\hat{c}^*$ .

Step 4: Repeat the above three steps  $B$  times, form a set of  $B$  bootstrapped replications of projection coefficient, and obtain bootstrap confidence intervals from bootstrap percentiles.

If the bootstrapped confidence interval of the projection coefficient does not include zero, we conclude the significant direction of  $\phi(\cdot)$  in its trend. If not, such direction is insignificant. We shall see in Section 5 that bootstrap inference on trend inference is empirically valid.

## 5 Simulation study

We present two simulation studies, first, to examine the finite sample behavior of the M-estimator by comparing the estimation accuracy of our marginal approach to that of existing functional approaches, and second, to investigate the performance of the bootstrap inference in trend test.

For the first simulation of comparative study, regular functional data, where each function shares a common range, are generated under six scenarios due to limited applicability of existing robust estimators to general data structures. We generate 80 independent curves following  $X(t) = \mu(t) + \sigma(t)\epsilon(t)$ ,  $t \in [0, 1]$ , for each scenario by varying assumptions on  $\sigma(t)$  or  $\epsilon(t)$ , or by adding artificial contamination under fixed smooth location function  $\mu(t)$ . Here,  $\sigma(t)$  represents magnitude of the noise and  $\epsilon(t)$  denotes the error process. The goal is the estimation of  $\mu(t)$  under various settings. For model 1-3, we generate data with the Gaussian,  $t_3$ , and Cauchy processes assumed on  $\epsilon(t)$ , respectively, with the constant  $\sigma(t) = 2$  over  $[0, 1]$ . The exponential spatial correlation structure is assumed on noise process, where  $\text{Cor}(\epsilon(t_1), \epsilon(t_2)) = \exp(-|t_1 - t_2|/d)$ . Here, the range parameter  $d$  determines

Table 1: Relative median ISE of the mean with respect to that of the proposed M-estimator under unscaled robust tuning parameter for models 1-6.

model1	model2	model3	model4	model5	model6
0.78	1.50	79.9	1.64	98.6	16.4



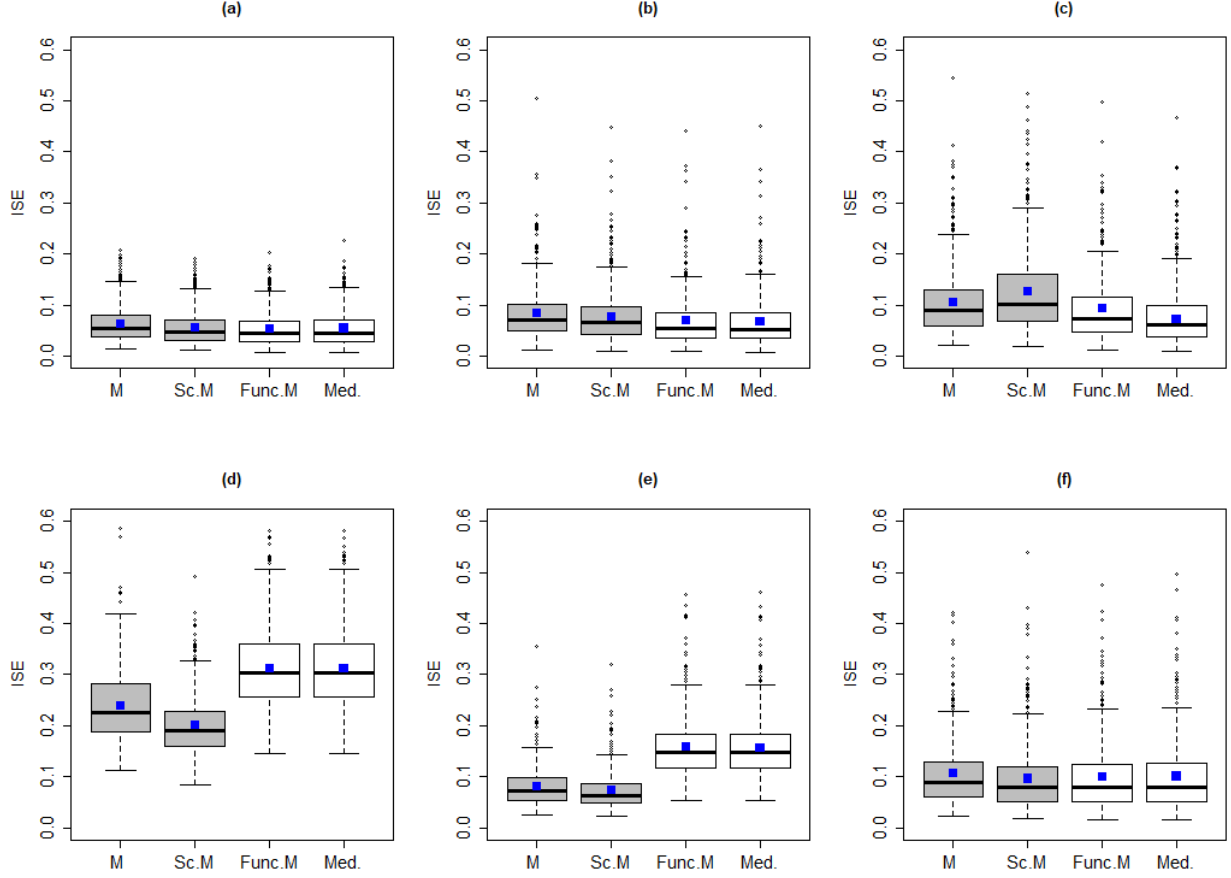


Figure 2: Boxplots of integrated squared error (ISE) over 500 replications from the marginal M-estimator (M), marginal scaled M-estimator (Sc.M), functional M-estimator (Func.M), and functional Median (Med.) under (a) Gaussian, (b)  $t_3$ , (c) Cauchy, (d) white-noise  $t_3$  with random scales, Gaussian partially contaminated by (e) Cauchy white-noise, and by (f) Cauchy processes. Blue square dots represent mean vales.

the spatial dependence within a curve and the value of 0.3 is used, but the studies with other values show the similar results. All curves are simulated at 100 equidistant points in  $[0, 1]$ . The model 4 considers the data with  $t_3$  white noise error with random scales, where  $\sigma(t)$ ,  $t \in [0, 1]$ , is generated from  $N(2, 10^2)$ . The model 5 and 6 generate the partially contaminated data, where  $X(t) = \mu(t) + \sigma(t)\epsilon(t)$ , for  $t \in [0, 0.2) \cup (0.4, 1]$ , under Gaussian process with the constant scale as in model 1-3, and  $X(t) = \mu(t) + \zeta(t)$ , for  $t \in [0.2, 0.4]$ .

For model 5, we consider Cauchy distributed white noise error process  $\zeta(t)$  with unit scale and, for model 6, Cauchy distributed contamination under exponential spatial correlation is assumed with unit scale. The generated data under six scenarios are illustrated in the supplementary material.

To calculate the proposed M-estimator, we adopt the Huber loss function and estimate the location parameter using constant or scaled robust tuning parameters. The former one uses the constant tuning parameter, say  $c$ , on  $t \in [0, 1]$ , and the latter one applies varying robust tuning parameters,  $c(t) = r * MAD(t)$ ,  $t \in [0, 1]$ , where  $r$  controls the overall robustness and  $MAD(t)$  indicates marginal median absolute deviation (MAD). In the simulation, we choose  $c$  as 0.8 to make the marginal estimates as close as marginal median values. For scaled approach, we set  $r = 0.2$  to make a fair comparison considering that  $\sigma = 2$ . For the comparative study, two competitors, a functional M-estimator developed by [Sinova et al. \(2018\)](#) and a functional median proposed by [Gervini \(2008\)](#) are considered. For the functional M-estimator by [Sinova et al. \(2018\)](#), we employ the same Huber loss function with a robust tuning parameter as 0.8. Lastly, the marginal mean is calculated to examine the effect of outlying curves in the estimation.

To evaluate the performance, the integrated square error (ISE) is calculated,  $ISE(\hat{\mu}) = \sum_{t=1}^{100} [\hat{\mu}(s_t) - \mu(s_t)]^2 / 100$ , over 500 repetitions, following [Sinova et al. \(2018\)](#) and Figure 2 presents boxplots of ISE from four estimators. The first two grey boxes represent results from the marginal M-estimators with ‘M’ and ‘Sc.M’ denoting M-estimator with constant tuning parameter and with the scaled tuning parameter. The ‘Func.M’ and ‘Med.’ indicate functional M-estimator from [Sinova et al. \(2018\)](#), and median from [Gervini \(2008\)](#). The results from the sample mean are excluded in visualization due to exceedingly large ISE’s. Instead, relative ratios of median ISE of the mean with respect to that of the proposed M-estimator are presented in Table 1. Similar relative ratios are found with respect to other robust estimators, thus they are not included in the paper. Under the Gaussian model (model 1), robust estimators achieve a similar estimation accuracy as functional mean does, but under the heavy-tailed or contaminated scenario, we observe the failure of

the sample mean with large ratios. Now, for the comparison among robust estimators in Figure 2, we see that under (a) Gaussian and (b)  $t_3$  errors, all four estimators achieve the almost similar estimation accuracy. Under (c) Cauchy noise, existing functional approaches slightly outperform, but it is not surprising because the discretized curves are generated under multivariate Cauchy distribution where the discretized functional approach is meant to be optimal. But the marginal approach still achieves comparable performance. Under the constant  $\sigma$  in model 1-3, M-estimator with constant tuning parameter seems slightly more stable than the estimator with a scaled parameter, but it does not seem to be a significant difference. The plot (d) displays the estimation error from the marginally independent noise and we see that two competitors fall behind the marginal approach in estimation accuracy. We observe the same pattern under the model of partial contamination by marginally independent Cauchy noise in (e). Under the spatially correlated contamination in (f), we again see a similar performance among four methods. Contrary to the comparable estimation errors among estimators under model 1-3, the distinction in performance is apparent under models 4 and 5. And, for the model of random noise scale, the M-estimator with scaled tuning parameter slightly outperforms one with unscaled parameter. In summary, our proposed marginal approach provides comparable or superior performances in estimation accuracy under various scenarios, compared to existing methods.

In the second simulation study, we investigate the validity of the bootstrap-based inference in functional trend test. The coverage probability and the length of the bootstrapped confidence intervals are investigated under five models and three sampling structures including partially observed framework. For the first three models, we borrow model 1-3 from the first simulation by assuming Gaussian,  $t_3$ , and Cauchy process, respectively, in error process, but with  $\mu(t) = \phi_0(t) + 2\phi_1(t) + 0.5\phi_2(t)$ ,  $t \in [0, 1]$ , where  $\phi_0(t)$ ,  $\phi_1(t)$ , and  $\phi_2(t)$  representing orthonormalized constant, linear, and quadratic basis functions, respectively. The other two models follow the contamination scenario in the first simulation, Gaussian curves contaminated by Cauchy process on  $[0, 0.3]$  and  $[0.7, 1]$ , respectively, with constant noise scale. For each scenario, 80 curves are generated at 100 equidistant

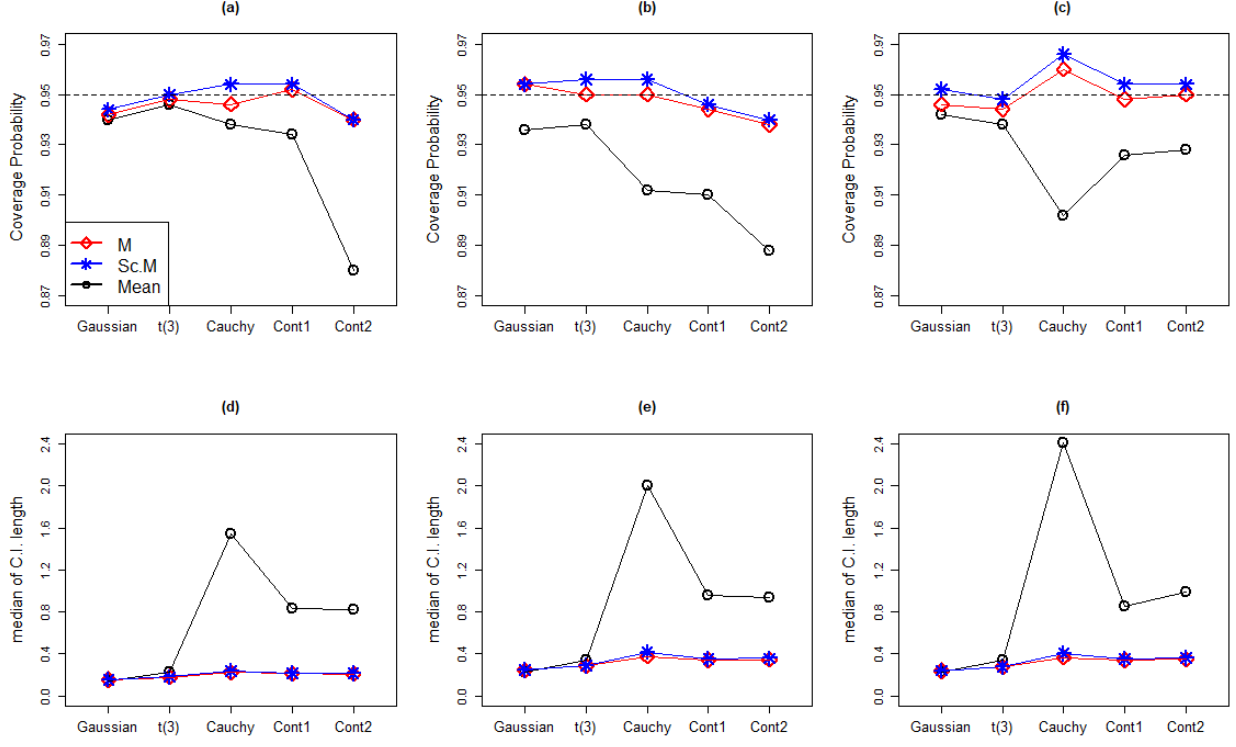


Figure 3: Coverage probabilities of bootstrapped confidence intervals of projection coefficients to quadratic function under Gaussian,  $t_3$ , Cauchy, and two contaminated data from M-estimator (M), scaled M-estimator (Sc.M), and Mean functions over 500 repetitions; (a) regular structure, partially observed structure under (b) random intervals, and under (c) under random but fixed number of intervals. Median length of bootstrapped confidence intervals of projection coefficient under (d) regular structure, partially observed structure under (e) random intervals, and under (f) random but fixed number of intervals

points over  $[0, 1]$ . Next, for five generated sets of curves, we apply three sampling frameworks; (i) regular data structure without missing, (ii) the partial sampling framework under random interval sampling, where,  $v_{1i}$  and  $v_{2i}$  being generated from  $\text{Beta}(0.3, 0.3)$ , and  $\delta_i(t) = \mathbf{1}_{\{t \in [\min(v_{i1}, v_{i2}), \max(v_{i1}, v_{i2})]\}}$ ,  $i = 1, \dots, 80$ , and (iii) random missing process but under fixed number of intervals, which randomly generates  $\delta_j(t)$ ,  $j = 1, 2, 3$ ,  $t \in [0, 1]$ , and randomly assign one of three to  $i$ th curve, for  $i = 1, \dots, 80$ . Note that we perform the

analysis hereafter for  $t \in [\varepsilon, 1 - \varepsilon]$  with  $\varepsilon = 0.01$  and scaled Beta distribution to ensure the Condition M3 as discussed in Section 2.1.

We calculate bootstrapped 95% confidence intervals of the projection coefficients to constant, linear, and quadratic functions under M-estimator, scaled M-estimator, and the sample mean function with 800 bootstrapped samples. Then the coverage probabilities are estimated from 500 repetitions based on the number of the inclusion of true coefficients in confidence intervals. Also, we calculate the median length of the intervals. All results are presented in the supplementary material and Figure 5 displays results from the projected coefficients to the quadratic trend. Plot (a), (b), and (c) illustrate the empirical coverage probabilities from regular, random interval sampling, and fixed interval sampling structures. We observe that the coverage probabilities from robust estimators are always around 95%. But, the overall probabilities from mean tend to be less than the desired 95%. Especially, under the Cauchy or contaminated model, inference from the functional mean may fail to detect the true quadratic trend. The plots of (d), (e), and (f) visualize the median length of confidence interval from each estimator, and the inference from functional mean seems less informative and unstable with the wide length of the interval. But the results from the proposed M-estimator seems stable regardless of distribution assumptions and missing structures.

## 6 Example: Quantitative Ultrasound Analysis

We illustrate the estimation of M-estimator and inference with the Quantitative Ultrasound (QUS) data. As introduced in Section 1, Wirtzfeld et al. (2015) presented data and results from diagnostic ultrasound studies using multiple transducers to scan mammary tumors (4T1) and benign fibrous masses (MAT) in rats and mice. In this experiment, total five transducers are used for noninvasive scan of each animal, and specifically, two transducers, 9L4 and 18L6, from Siemens, cover 310.8 MHz, L14-5 from Ultrasonix uses frequencies 38.5 MHz, and MS200 and MS400 from VisualSonics cover higher frequencies, 8.513.5 MHz, and

8.521.9 MHz.

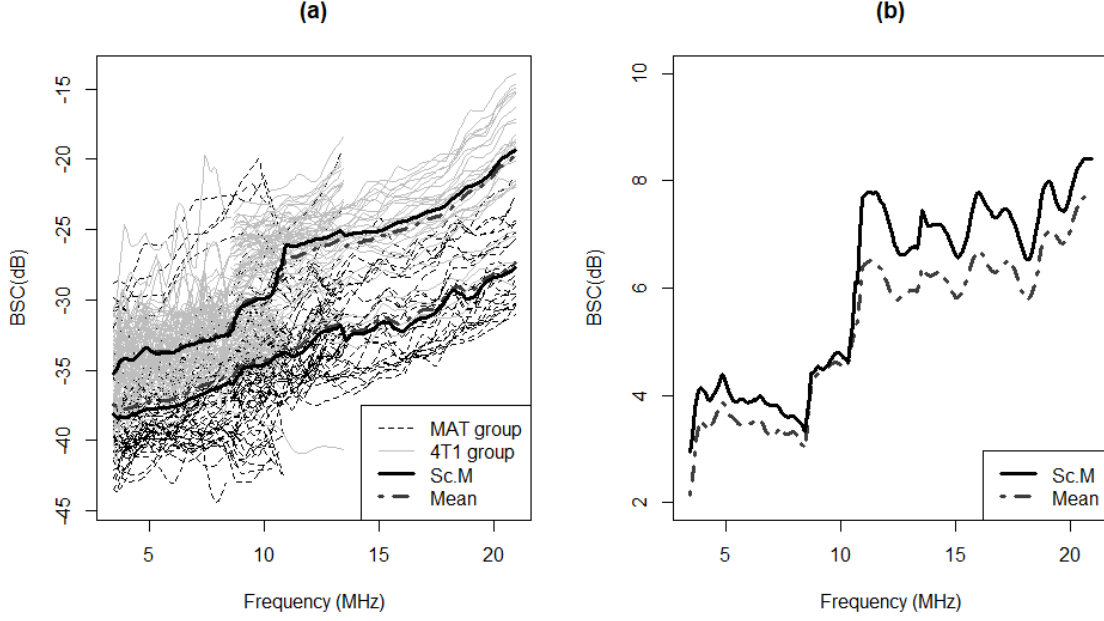


Figure 4: Quantitative Ultrasound data. (a) BSC curves from MAT and 4T1 tumors with proposed functional M-estimator and functional mean for each group. (b) Marginal group differences of M-estimator and mean.

The aims of this experiment are the detection of significant differences in the behavior of BSC curves between two distinct tumors and investigation of the consistency among frequency ranges or transducers in such detection. To address this, we calculate the functional M-estimator and derive inferential statistic on functional trend. Figure 4 (a) shows estimated group location parameters from marginal M-estimator under Huber loss with a scaled robust tuning parameter and from the functional mean for two tumor types. We observe remarkable jumps at 8.5 MHz and 10.8 MHz in a group of the 4T1 tumor and they are corresponding to frequencies where a change in the variety of transducers is observed. But the jump on functional mean at 10.8 MHz is weaker than the jump on M-estimator due to multiple outlying curves in the 4T1 group which have suspiciously small values or abnormal behaviors comparing to the majority.

Figure 4 (b) presents the marginal differences between two tumor group locations to examine the trend in tumor detection. Seemingly, an increasing trend is detected, but the inferential justification is needed to make a conclusion. It can be related to functional ANOVA, but our interest is not only in the detection of significant distinction in location parameters but also in the detection of a significant trend over frequencies to address the effect of transducers or frequency ranges. To this end, we calculate bootstrapped confidence intervals of projection coefficients corresponding to the selected basis functions. We specifically consider constant, linear, and quadratic basis functions as well as three step functions, named as Step1, Step2, and Step3, where Step1 has a jump at 8.5 MHz, Step2 has a jump at 10.8 MHz, and Step3 at 13.5 MHz. Step functions are defined based on known transducer information. The inferences based on coefficients of the first three basis functions enable identifying a general trend, whether higher frequencies separate two groups more efficiently than lower frequencies do. Meanwhile, coefficients of three step functions provide information to discover the transducer effect. We adopt the Huber function in M-estimator with constant and scaled robust tuning parameters as discussed in Section 5.

Table 2: Estimated projection coefficients to basis functions. 95% and 99% bootstrapped confidence intervals in round brackets and square brackets, respectively. Bracket with \* indicates an interval not including zero in it.

	Quadratic	Linear	Constant	Step1	Step2	step3
M-estimator	-0.15	1.55	6.00	0.22	0.66	-0.11
	(-0.52, 0.17)	(0.54, 2.38)*	(4.90, 6.97)*	(-0.05, 0.52)	(0.29, 1.00)*	(-0.46, 0.31)
	[-0.65, 0.29]	[0.18, 2.63]*	[4.51, 7.20]*	[-0.14, 0.64]	[0.18, 1.09]*	[-0.65, 0.44]
Scaled M-estimator	-0.22	1.48	5.98	0.24	0.58	-0.06
	(-0.50, 0.11)	(0.56, 2.31)*	(4.88, 6.91)*	(-0.01, 0.49)	(0.27, 0.86)*	(-0.42, 0.26)
	[-0.61, 0.23]	[0.20, 2.55]*	[4.50, 7.15]*	[-0.10, 0.56]	[0.17, 0.97]*	[-0.55, 0.40]
Mean	-0.16	1.32	5.28	0.24	0.34	-0.07
	(-0.44, 0.15)	(0.58, 2.05)*	(4.33, 6.13)*	(0.02, 0.46)*	(0.05, 0.62)*	(-0.38, 0.25)
	[-0.53, 0.24]	[0.30, 2.29]*	[4.07, 6.35]*	[-0.05, 0.52]	[-0.02, 0.71]	[-0.47, 0.32]

For unscaled one, we choose  $c = 0.8$ , and for the scaled one,  $r = 0.4$  with the consideration of the overall estimated MAD over the whole frequency range.

Table 2 shows estimated coefficients of functional group difference projected to six basis functions and corresponding 95% and 99% bootstrapped confidence intervals based on 3000 replications. The discretized curves in the data are densely collected but do not share common grids, so interpolation is applied to each curve at an equally spaced grid of 176 points over 3-21.6 MHz. The computation time on 3.60GHz Intel(R) Core(TM) i7-7700 CPU is 234 seconds for derivation of bootstrapped confidence intervals from M-estimator with  $n_{4T1} = 115$ ,  $n_{MAT} = 149$ . First, we observe that results of M-estimator from scaled and constant tuning parameters look almost the same except the discrepancy in estimated coefficients of the quadratic term. But the quadratic trend is insignificant from both bootstrapped inferences, so fundamentally two estimators derive the same conclusion. Then a significant linear trend is detected in group differences with positive coefficients from M-estimator, which implies that higher frequencies are more efficient to detect group differences than lower frequencies are. The finding is the same for the mean approach, but shrunk estimate is observed due to the effect of outliers. To examine the transducer effect, we see results from three step functions. Change point at 8.5 MHz (Step1) turns out to be insignificant from robust estimators, but 95% confidence interval from mean does not include zero, implying significant distinct behavior at this jump. For the second change point, robust M-estimators detect significant positive jump at 10.8 MHz with confidence, with the lower bound far from zero, but the inference from mean function fails to detect such change in 99% confidence interval. Although inference from 95% confidence interval detects significant jump, it lacks confidence with lower bound very close to zero. Again, this different conclusion is due to multiple outliers in the 4T1 group and mean function underestimates the jump at this change point. The last change point between two Visual-Sonics transducers turns out to be insignificant from both estimators. In conclusion, BSC curves significantly distinct different tumors along with all frequency ranges and higher frequencies separate them more efficiently than lower frequencies do. Furthermore, we



see a significant positive jump at 10.8 MHz, which implies the outperformed efficiency of VisualSonics transducers in terms of tissue distinction comparing to others.

## 7 Concluding Remarks

We propose a class of robust M-estimator applicable to partially observed functional data. We show that our estimator is consistent and asymptotically follows the Gaussian process with root- $n$  rates of convergence under a key condition for sup-norm convergence of the indicator process. Also, a functional trend test tool is developed based on asymptotic normality and it can be performed in practice with a bootstrap approach. The validity of bootstrap inference is supported by simulation studies, where the true trend is detected with the desired coverage probability under heavy-tailed or contaminated distribution and various structures of missingness. In terms of estimation accuracy, numerical simulation experiments demonstrate how the proposed estimator can outperform existing functional robust estimators, even in the case of complete data.

## References

- Cuevas, A., Febrero-Bande, M., & Fraiman, R. (2007). Robust estimation and classification for functional data via projection-based depth notions. *Computational Statistics*, 22, 481–496.
- Delaigle, A. & Hall, P. (2013). Classification using censored functional data. *Journal of the American Statistical Association*, 108, 1269–1283.
- Delaigle, A. & Hall, P. (2016). Approximating fragmented functional data by segments of markov chains. *Biometrika*, 103, 779—799.
- Fraiman, R. & Muniz, G. (2001). Trimmed means for functional data. *Test*, 10, 419–440.

- Gellar, J. E., Colantuoni, E., Needham, D. M., & Crainiceanu, C. M. (2014). Variable-domain functional regression for modeling icu data. *Journal of the American Statistical Association*, 109, 1425–1439.
- Gervini, D. (2008). Robust functional estimation using the median and spherical principal components. *Biometrika*, 95, 587–600.
- Goldberg, Y., Ritov, Y., & Mandelbaum, A. (2014). Predicting the continuation of a function with applications to call center data. *Journal of Statistical Planning and Inference*, 147, 53–65.
- Gromenko, O., Kokoszka, P., & Sojka, J. (2017). Evaluation of the cooling trend in the ionosphere using functional regression with incomplete curves. *The Annals of Applied Statistics*, 11, 898–918.
- Hampel, F. R. (1974). The influence curve and its role in robust estimation. *Journal of the American Statistical Association*, 69, 383–393.
- Horváth, L. & Kokoszka, P. (2012). *Inference for Functional Data with Applications*. Springer.
- Hsing, T. & Eubank, R. (2015). *Theoretical Foundations of Functional Data Analysis, with an Introduction to Linear Operators*. John Wiley & Sons.
- Huber, P. (2005). *Robust Statistics*. John Wiley & Sons.
- Kneip, A. & Liebl, D. (2019). On the optimal reconstruction of partially observed functional data. *Annals of Statistics*, *In press*.
- Kraus, D. (2015). Components and completion of partially observed functional data. *Journal of the Royal Statistical Society, Series B*, 77, 777–801.
- Kraus, D. (2019). Inferential procedures for partially observed functional data. *Journal of Multivariate Analysis*, 173, 583–603.

- Kraus, D. & Stefanucci, M. (2018). Classification of functional fragments by regularized linear classifiers with domain selection. *Biometrika*, 106, 161–180.
- Liebl, D. (2013). Modeling and forecasting electricity spot prices: A functional data perspective. *The Annals of Applied Statistics*, 7, 1562–1592.
- Locantore, N., Marron, J. S., Simpson, D. G., Tripoli, N., Zhang, J., & Cohen, K. L. (1999). Robust principal component analysis for functional data (with discussion). *Test*, 8, 1–73.
- López-Pintado, S. & Romo, J. (2009). On the concept of depth for functional data. *Journal of the American Statistical Association*, 104, 718–734.
- López-Pintado, S. & Romo, J. (2011). A half-region depth for functional data. *Computational Statistics and Data Analysis*, 55, 1679–1695.
- Mojirsheibani, M. & Shaw, C. (2018). Classification with incomplete functional covariates. *Statistics & Probability Letters*, 139, 40–46.
- Park, Y. (2017). *Effect size estimation and robust classification for irregularly sampled functional data*. PhD thesis, University of Illinois at Urbana-Champaign. <http://hdl.handle.net/2142/98126>.
- Park, Y. & Simpson, D. G. (2019). Robust probabilistic classification applicable to irregularly sampled functional data. *Computational Statistics and Data Analysis*, 131, 37–49.
- Ramsay, J. & Silverman, B. W. (2005). *Functional Data Analysis*. Springer.
- Sinova, B., González-Rodríguez, Gil, & Van Aelst, S. (2018). M-estimators of location for functional data. *Bernoulli*, 24(3), 2328–2357.
- Stefanucci, M., Sangalli, L. M., & Brutti, P. (2018). Pcabased discrimination of partially observed functional data, with an application to aneurisk65 data set. *Statistica Neerlandica*, 72, 246–264.

van der Vaart, A. & Wellner, J. (1996). *Weak Convergence and Empirical Processes: With Applications to Statistics*. Springer.

van der Vaart, A. W. (2007). *Asymptotic Statistics*. Cambridge University Press.

Vershynin, R. (2019). *High-Dimensional Probability*. Cambridge Series in Statistical and Probabilistic Mathematics (Book 47). Cambridge University Press.

Wirtzfeld, L. A., Ghoshal, G., Rosado-Mendez, I. M., Nam K., Park, Y., Pawlicki, A., Miller, R. J., Simpson, D. G., Zagzebski, J. A., Oelze, M. L., Hall, T. J., & O' Brien, W. D. (2015). Quantitative ultrasound comparison of mat and 4t1 mammary tumors in mice and rats across multiple imaging systems. *Journal of Ultrasound in Medicine*, 34, 1373–1383.

## A Proofs

Proof of Proposition 2.1. Under M1, M4, A1-A3, we write the pdf of the marginal distribution of  $Y$  at  $t \in \mathbb{C}$  as  $f(y)$  and it is assumed to be symmetric (or even function) about  $\alpha(t)$ . Then

$$E_{P_Y}[\psi(Y(t) - \alpha(t))] = \int_{-\infty}^{\infty} \psi(Y(t) - \alpha(t))f(Y(t) - \alpha(t))dy = 0, \quad t \in \mathbb{C},$$

under the assumption of even function  $\psi(\cdot)$ . Thus,  $\theta(t) = \alpha(t)$ .  $\square$

Proof of Proposition 2.2. Under A1-A3, M4, equation (5) is equivalently written as  $E_{P_Y}[\psi(Y(t) - \alpha(t) + \alpha(t) - \theta(t))] = 0$ . And, under B1, the marginal distribution of  $Y(t) - \alpha(t)$ ,  $t \in \mathbb{C}$ , does not depend on  $t$  with the probability measure  $P_Z$ . Then  $\theta(t)$  satisfies

$$E_{P_Z}[\psi(Z - \{\alpha(t) - \theta(t)\})] = 0,$$

and  $\{\alpha(t) - \theta(t)\} = c$ , where constant  $c$  is determined by  $P_Z$ . Thus,  $\theta(t) = \alpha(t) + c$ .  $\square$

Proof of Theorem 2.3. Denote  $T(P_\varepsilon)(t)$  by  $\theta_\varepsilon(t)$ . Under D2, for any  $v > 0$ , there exists  $\delta > 0$ ,

$$\begin{aligned}
P(\sup_{t \in C} |\theta_\varepsilon(t) - \theta(t)| > v) &\leq P(\sup_{t \in C} [M(t, \theta_\varepsilon, P) - M(t, \theta, P)] > \delta) \\
&\leq P(\sup_{t \in C} [M(t, \theta_\varepsilon, P) - M(t, \theta_\varepsilon, P_\varepsilon) + M(t, \theta, P_\varepsilon) - M(t, \theta, P)] > \delta) \\
&\leq P(\sup_{t \in C} |M(t, \theta_\varepsilon, P) - M(t, \theta_\varepsilon, P_\varepsilon)| > \delta/2) \\
&\quad + P(\sup_{t \in C} |M(t, \theta, P_\varepsilon) - M(t, \theta, P)| > \delta/2).
\end{aligned}$$

By D1,  $T(P_\varepsilon)(t)$  is uniformly continuous as  $\varepsilon \rightarrow 0$ . □

Proof of Theorem 2.4. By the estimating equation of (5),

$$\begin{aligned}
0 &= (1 - \varepsilon)E_P[\delta(t)\psi(Y(t), \theta_\varepsilon(t))] + \varepsilon\delta^*(t)\psi(Y^*(t), \theta_\varepsilon(t)) \\
&= (1 - \varepsilon)E_P[\delta(t)\{\psi(Y(t), \theta_\varepsilon(t)) - \psi(Y(t), \theta(t))\}] + \varepsilon\delta^*(t)\psi(Y^*(t), \theta_\varepsilon(t)) \\
&= (1 - \varepsilon)E_P[\delta(t)\frac{\psi(Y(t), \theta_\varepsilon(t)) - \psi(Y(t), \theta(t))}{\varepsilon}] + \delta^*(t)\psi(Y^*(t), \theta_\varepsilon(t))
\end{aligned}$$

Let  $\varepsilon \rightarrow 0$ , then

$$0 = E_P[\delta(t)\dot{\psi}(Y(t), \theta(t))] \dot{\theta}(t) + \delta^*(t)\psi(Y^*(t), \theta(t)).$$

Thus,

$$\dot{\theta}(t) = IF_T(Y^*, \delta^*)(t) = \frac{\delta^*(t)\psi(Y^*(t) - \theta(t))}{-E_P[\delta(t)\dot{\psi}(Y(t), \theta(t))]},$$

and the bounded  $\psi(\cdot)$  implies  $\gamma_T^\infty < \infty$ . □

Proof of Lemma 3.1. In this proof, we shall use  $C > 0$  to denote generic constants whose values may change from line to line. Since  $C$  is compact in  $\mathbb{R}$ , we may assume that, without loss of generality,  $C \subseteq [0, 1]$ . Let  $s, t \in [0, 1]$  and denote  $\eta_i(s, t) = [\delta_i(s) - \delta_i(t)] - [b(s) - b(t)]$ . Note that, for each fixed  $s$  and  $t$ , the random variables  $\eta_i$  are mean-zero i.i.d. with bounded ranges  $[-2, 2]$ . By Bernstein's inequality (cf. Lemma 2.2.9 in [van der Vaart & Wellner \(1996\)](#)), we have for any  $\varepsilon > 0$ ,

$$P(|\sum_{i=1}^n \eta_i(s, t)| > \varepsilon) \leq 2 \exp\left(-\frac{\varepsilon^2/2}{V_n + 2\varepsilon/3}\right),$$

where

$$V_n(s, t) = \sum_{i=1}^n \mathbb{E}[\eta_i(s, t)^2] = n \text{Var}(\eta_i) = n[c(s, s) + c(t, t) - 2c(s, t)].$$

By Lemma A.1, there exists an absolute constant  $C > 0$  such that

$$\left\| \sum_{i=1}^n \eta_i(s, t) \right\|_{\psi_1} \leq C \sqrt{n} d(s, t),$$

where  $d(s, t)^2 = c(s, s) + c(t, t) - 2c(s, t)$ . Let

$$X_t = \frac{1}{\sqrt{n}} \sum_{i=1}^n [\delta_i(t) - b(t)].$$

be an empirical process indexed by  $t \in [0, 1]$ . Then for any  $s, t \in [0, 1]$ ,

$$\|X_s - X_t\|_{\psi_1} \leq C d(s, t),$$

which shows that  $(X_t)_{t \in [0, 1]}$  is a sub-exponential process. By Condition M2, we have  $d(s, t) \asymp |s - t|^2$ , which implies that

$$N([0, 1], d, \varepsilon) \leq C N([0, 1], |\cdot|, \varepsilon).$$

Then Dudley's entropy integral bound for  $\psi_1$ -norm (cf. Corollary 2.2.5 in [van der Vaart & Wellner \(1996\)](#)) yields that

$$\mathbb{E} \left[ \sup_{t \in [0, 1]} X_t \right] \leq C \int_0^1 \log N([0, 1], |\cdot|, \varepsilon) d\varepsilon,$$

By Corollary 4.2.13 in [Vershynin \(2019\)](#), we have

$$N([0, 1], |\cdot|, \varepsilon) \leq \left(1 + \frac{2}{\varepsilon}\right) \leq \left(\frac{3}{\varepsilon}\right), \quad \forall \varepsilon \in (0, 1].$$

Combining the last two inequalities, we get

$$\mathbb{E} \left[ \sup_{t \in [0, 1]} X_t \right] \leq C \int_0^1 \log \left( \frac{3}{\varepsilon} \right) d\varepsilon \leq C,$$

where the last inequality follows from integration-by-parts. Since  $W_n \leq 2n^{-1/2} \sup_{t \in [0, 1]} X_t$ , the lemma follows.  $\square$

**Lemma A.1** ( $\psi_1$ -norm bound for sub-exponential random variables). *Let  $X$  be a mean-zero random variable satisfying a Bernstein-type inequality: there is a constant  $C_1 > 0$  such that for any  $t > 0$ ,*

$$P(|X| \geq t) \leq 2 \exp[-C_1 \min(t^2/V, t)].$$

Then,

$$\|X\|_{\psi_1} \leq C_2 V^{1/2},$$

where  $C_2 > 0$  is a constant only depending on  $C_1$ .

*Proof of Lemma A.1.* Let  $C > 0$  be a large enough constant depending only on  $C_1$ . By integration-by-parts and change-of-variables, we have

$$\begin{aligned} \mathbb{E} \left[ \exp \left( \frac{|X|}{C} \right) \right] &= \int_1^\infty P \left( \exp \left( \frac{|X|}{C} \right) > t \right) dt \\ &= \int_1^\infty P(|X| > C \log t) dt \\ &= \int_0^\infty P(|X| > Cx) e^x dx \\ &\leq 2 \int_0^{p/C} e^{-\frac{C_1 C^2}{V} x^2 + x} dx + 2 \int_{V/C}^\infty e^{-(C_1 C - 1)x} dx \\ &\leq 2 e^{\frac{V}{4C_1 C^2}} \sqrt{\frac{\pi V}{C_1 C^2}} + \frac{2}{C_1 C - 2} e^{-(C_1 C - 2)\frac{V}{C}}. \end{aligned}$$

Thus if we take  $C = KV^{1/2}$  for some large enough constant  $K := K(C_1) > 0$ , then

$$\mathbb{E} \left[ \exp \left( \frac{|X|}{C} \right) \right] \leq 2,$$

which implies that  $\|X\|_{\psi_1} \leq KV^{1/2}$ . □

*Proof of Theorem 3.2.* For  $t \in \mathbb{C}$ , if  $|\hat{\theta}_n(t) - \theta(t)| > \epsilon$ , then  $M(t, \hat{\theta}_n, P) - M(t, \theta, P) > \delta_t$

by D2, and  $\sup_t [M(t, \hat{\theta}_n, P) - M(t, \theta, P)] > \delta$ , where  $\delta = \sup_t \delta_t$ . Then

$$\begin{aligned}
P(\sup_{t \in C} |\hat{\theta}_n(t) - \theta(t)| > \epsilon) &\leq P(\sup_{t \in C} [M(t, \hat{\theta}_n, P) - M(t, \theta, P)] > \delta) \\
&= P(\sup_{t \in C} [M(t, \hat{\theta}_n, P) - M(t, \hat{\theta}_n, P_n) + M(t, \hat{\theta}_n, P_n) - M(t, \theta, P_n) \\
&\quad + M(t, \theta, P_n) - M(t, \theta, P)] > \delta) \\
&\leq P(\sup_{t \in C} [M(t, \hat{\theta}_n, P) - M(t, \hat{\theta}_n, P_n) + M(t, \theta, P_n) - M(t, \theta, P)] > \delta) \\
&\leq P(\sup_{t \in C} |M(t, \hat{\theta}_n, P) - M(t, \hat{\theta}_n, P_n)| > \delta/2) \\
&\quad + p(\sup_{t \in C} |M(t, \theta, P_n) - M(t, \theta, P)| > \delta/2)
\end{aligned}$$

By D1,  $\hat{\theta}_n(t)$  uniformly converges to  $\theta(t)$  over  $C$  as  $n \rightarrow \infty$ .  $\square$

*Proof of Theorem 3.3.* Let  $\tilde{Z}_n(t) = n^{-1/2} \sum_{i=1}^n \delta_i(t) V_i(t) / b(t)$ . For any  $t_1, \dots, t_K \in C$ , denote  $\tilde{\mathbf{Z}}_n = (\tilde{Z}_n(t_1), \dots, \tilde{Z}_n(t_K))^T$ . By the multivariate CLT and the independence between  $\delta_i$  and  $V_i$ , we have

$$\tilde{\mathbf{Z}}_n \xrightarrow{d} N(0, \Xi),$$

where  $\Xi = \{\vartheta_{jk}\}_{j,k=1}^K$  is the  $K \times K$  covariance matrix with  $\vartheta_{jk} = v(t_j, t_k) \gamma(t_j, t_k) / [b(t_j) b(t_k)]$ . By Theorem 7.4.2 in [Hsing & Eubank \(2015\)](#), the process  $\{\tilde{Z}_n(t) : t \in C\}$  is a random element in the Hilbert space  $\mathbb{H} = L^2(C, \mathcal{B}(C), \mu)$ , where  $\mu$  is a finite measure on  $C$ . Then it follows from Theorem 7.7.6 in [Hsing & Eubank \(2015\)](#) for i.i.d. Hilbert space valued random variables that

$$\{\tilde{Z}_n(t) : t \in C\} \rightsquigarrow \text{GP}(0, \vartheta),$$

where the finite-dimensional restrictions of  $\vartheta$  is given by the covariance matrix  $\Xi$ . Note that

$$\sup_{t \in C} |\tilde{Z}_n(t) - Z_n(t)| \leq \sup_{t \in C} |\tilde{Z}_n(t)| \cdot \sup_{t \in C} \left| 1 - \frac{b(t)}{\bar{\delta}_n(t)} \right|,$$

where  $\bar{\delta}_n(t) = n^{-1} \sum_{i=1}^n \delta_i(t)$ . Note that

$$|\bar{\delta}_n(t)| \geq b(t) - |\bar{\delta}_n(t) - b(t)| \geq \inf_{t \in C} b(t) - W_n,$$



where

$$W_n = \sup_{t \in \mathbb{C}} |n^{-1} \sum_{i=1}^n [\delta_i(t) - b(t)]|.$$

By Lemma 3.1,  $E[W_n] = O(n^{-1/2})$ . Since  $\sup_{t \in \mathbb{C}} |\tilde{Z}_n(t)| = O_P(1)$ , we have

$$\sup_{t \in \mathbb{C}} |\tilde{Z}_n(t) - Z_n(t)| = O_P(n^{-1/2}).$$

Then Theorem 3.3 is an immediate consequence of Slutsky's lemma.  $\square$

Proof of Theorem 3.4. The estimating equation (3) can be equivalently written as,

$$\frac{1}{\sum_{j=1}^n \delta_j(t)} \sum_{i=1}^n \delta_i(t) \psi(Y_i(t), \hat{\theta}_n(t)) = 0.$$

By mean value theorem,

$$\frac{1}{\sum_{j=1}^n \delta_j(t)} \sum_{i=1}^n \delta_i(t) \psi(Y_i(t), \theta(t)) + \frac{1}{\sum_{j=1}^n \delta_j(t)} \sum_{i=1}^n \delta_i(t) \dot{\psi}(Y_i(t), \tilde{\theta}_n(t)) (\hat{\theta}_n(t) - \theta(t)) = 0,$$

where  $\theta(t) \leq \tilde{\theta}_n(t) \leq \hat{\theta}_n(t)$ ,  $t \in \mathbb{C}$ . Rearranging terms, we get

$$\sqrt{n}(\hat{\theta}_n(t) - \theta(t)) = - \underbrace{\left[ \frac{1}{\sum_{j=1}^n \delta_j(t)} \sum_{i=1}^n \delta_i(t) \dot{\psi}(Y_i(t), \tilde{\theta}_n(t)) \right]^{-1}}_{(1)} \underbrace{\frac{1}{\sum_{j=1}^n \delta_j(t)} \sqrt{n} \sum_{i=1}^n \delta_i(t) \psi(Y_i(t), \theta(t))}_{(2)},$$

where

$$\begin{aligned} (1) &= \frac{1}{\sum_{j=1}^n \delta_j(t)} \sum_{i=1}^n \delta_i(t) \left[ \dot{\psi}(Y_i(t), \tilde{\theta}_n(t)) - \dot{\psi}(Y_i(t), \theta(t)) \right] + \frac{1}{\sum_{j=1}^n \delta_j(t)} \sum_{i=1}^n \delta_i(t) \dot{\psi}(Y_i(t), \theta(t)) \\ &= \frac{1}{\sum_{j=1}^n \delta_j(t)/n} \sum_{i=1}^n \left[ \frac{\delta_i(t)}{n} - \frac{b(t)}{n} \right] \left[ \dot{\psi}(Y_i(t), \tilde{\theta}_n(t)) - \dot{\psi}(Y_i(t), \theta(t)) \right] \\ &\quad + \frac{b(t)}{\sum_{j=1}^n \delta_j(t)/n} \left[ \frac{1}{n} \sum_{i=1}^n \dot{\psi}(Y_i(t), \tilde{\theta}_n(t)) - \dot{\psi}(Y_i(t), \theta(t)) \right] + \frac{1}{\sum_{j=1}^n \delta_j(t)} \sum_{i=1}^n \delta_i(t) \dot{\psi}(Y_i(t), \theta(t)) \\ &\leq \sup_{t \in \mathbb{C}} \left\{ \frac{1}{\sum_{j=1}^n \delta_j(t)/n} \right\} \sup_{t \in \mathbb{C}} \left| \sum_{i=1}^n \left[ \frac{\delta_i(t)}{n} - \frac{b(t)}{n} \right] \left[ \dot{\psi}(Y_i(t), \tilde{\theta}_n(t)) - \dot{\psi}(Y_i(t), \theta(t)) \right] \right| \\ &\quad + \sup_{t \in \mathbb{C}} \left\{ \frac{b(t)}{\sum_{j=1}^n \delta_j(t)/n} \right\} \sup_{t \in \mathbb{C}} \left| \frac{1}{n} \sum_{i=1}^n \dot{\psi}(Y_i(t), \tilde{\theta}_n(t)) - \dot{\psi}(Y_i(t), \theta(t)) \right| \\ &\quad + \frac{1}{\sum_{j=1}^n \delta_j(t)} \sum_{i=1}^n \delta_i(t) \dot{\psi}(Y_i(t), \theta(t)). \end{aligned}$$

As  $n \rightarrow \infty$ , under given conditions, Lemma 3.1, and Theorem 3.2, it is  $O_P(n^{-1/2}) + o_P(1) + E_{P_Y} \dot{\psi}(Y_1(t), \theta(t))$ . By Theorem 3.3, term (2) converges to Gaussian Process with mean zero and covariance function  $\varphi(s, t) = \text{Cov} \{ \psi(Y(t), \theta(t)), \psi(Y(s), \theta(s)) \} \frac{v(s, t)}{b(s)b(t)}$ , where  $v(s, t) = E_{P_\delta}[\delta(s)\delta(t)]$ . Then Theorem 3.4 is an immediate consequence of Slutsky's lemma.  $\square$

Proof of Corollary 3.5. By Karhuneun-Loéve theorem,  $\xi(s, t) = \sum_{r=1}^k \lambda_r e_r(t) e_r(s)$  and we have  $\sqrt{n}(\hat{\theta}_n(t) - \theta(t)) = \sum_{r=1}^k \eta_r e_r(t)$ , where

$$\eta_r = \int_C \sqrt{n}(\hat{\theta}_n(t) - \theta(t)) e_r(t) dt \sim AN(0, \lambda_r), \quad r = 1, \dots, k.$$

Then we can write

$$\begin{aligned} \sqrt{n} \langle (\hat{\theta}_n(\cdot) - \theta(\cdot)), \phi(\cdot) \rangle &= \sqrt{n} \left( \langle \hat{\theta}_n(t), \phi(\cdot) \rangle - c \right) = \int \left( \sum_{r=1}^k \eta_r e_r(t) \right) \phi(t) dt \\ &= \sum_{r=1}^k \eta_r \int e_r(t) \phi(t) dt = \sum_{r=1}^k \eta_r \langle e_r(\cdot), \phi(\cdot) \rangle, \end{aligned}$$

Under the assumption of  $tr(\xi) < \infty$ ,  $\sum_{r=1}^k \eta_r$  converges in distribution especially to normal distribution. Thus,  $\sum_{r=1}^k \eta_r \langle e_r(\cdot), \phi(\cdot) \rangle$  also converges to normal distribution under  $\langle e_r(t), \phi(t) \rangle < \|e_r(t)\| \cdot \|\phi(t)\| = c < \infty$ . The asymptotic variance is derived as,

$$\tau^2 = \text{Var} \{ \langle \sqrt{n}(\hat{\theta}_n(\cdot) - \theta(\cdot)), \phi(\cdot) \rangle, \langle \sqrt{n}(\hat{\theta}_n(\cdot) - \theta(\cdot)), \phi(\cdot) \rangle \} = \int \int_C \phi(s) \xi(s, t) \phi(t) ds dt.$$

$\square$

Proof of Proposition 4.1. For  $t \in C$ ,

$$\begin{aligned} \text{Cov}(Y_i^*(t), \delta_i^*(t)) &= \text{Cov}(\mathbf{U}_i^T Y(t), \mathbf{U}_i^T \delta(t)) = \mathbf{X}^T(t) \text{Cov}(\mathbf{U}_i) \boldsymbol{\delta}(t) \\ &= \sum_i Y_i(t) \delta_i(t) / n - \left( \sum_i Y_i(t) / n \right) \left( \sum_i \delta_i(t) / n \right), \end{aligned} \tag{10}$$

as  $n \rightarrow \infty$ , it approximates to  $E[Y_i(t)\delta_i(t)] - E[Y_i(t)]E[\delta_i(t)]$ , for each  $t \in C$ , which is zero.  $\square$

## B Appendix

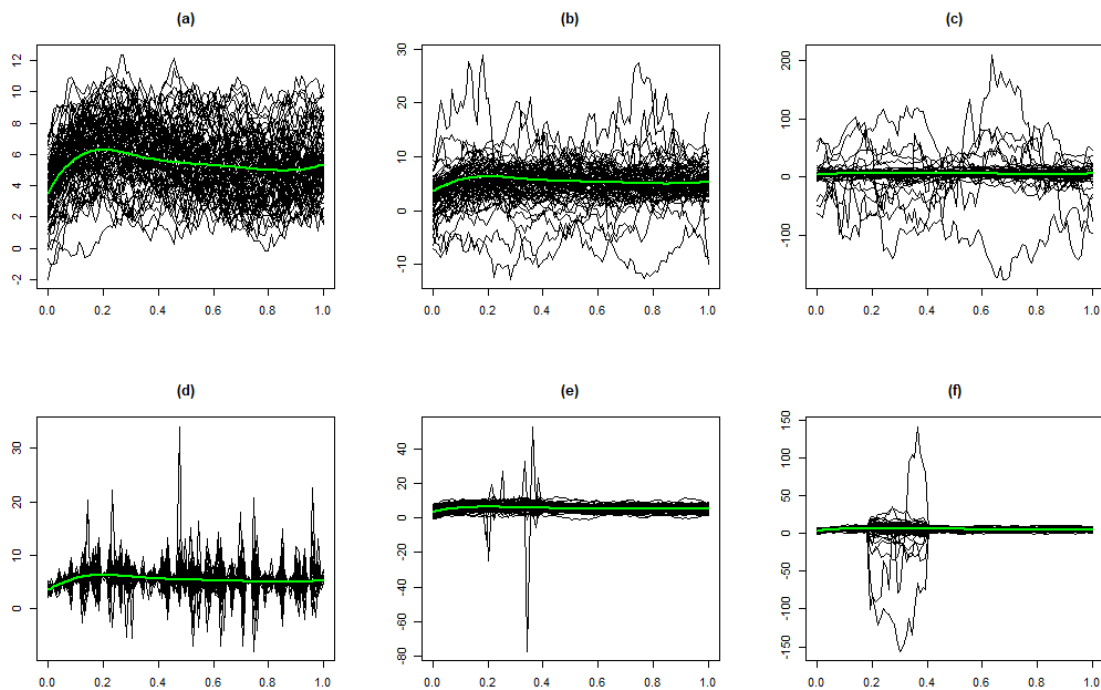


Figure 5: Simulated data from the scenario of (a) Gaussian, (b)  $t_3$ , (c) Cauchy, (d) white-noise  $t_3$  with random scales, Gaussian partially contaminated by (e) Cauchy white-noise, and by (f) Cauchy processes. Green line indicates location function.

Table 3: Coverage probabilities and the median length of bootstrapped confidence intervals (in parenthesis) of projection coefficient to quadratic basis function from M-estimator (M), scaled M-estimator (Sc.M), and mean over 500 repetitions

	Regular			Irregular1			Irregular2		
	Mean	Mt	Sc.M	Mean	M	Sc.Mt	Mean	M	Sc.M
Gaussian	0.94	0.942	0.942	0.936	0.954	0.954	0.942	0.946	0.952
	(0.14)	(0.15)	(0.15)	(0.23)	(0.24)	(0.24)	(0.22)	(0.24)	(0.24)
t(3)	0.46	0.948	0.95	0.94	0.95	0.95	0.938	0.944	0.948
	(0.23)	(0.18)	(0.18)	(0.35)	(0.29)	(0.29)	(0.35)	(0.28)	(0.28)
Cauchy	0.938	0.946	0.954	0.912	0.950	0.956	0.902	0.960	0.966
	(1.55)	(0.22)	(0.24)	(2.00)	(0.37)	(0.42)	(2.41)	(0.37)	(0.40)
Cont.1	0.934	0.952	0.954	0.910	0.944	0.946	0.926	0.948	0.954
	(0.83)	(0.21)	(0.22)	(0.95)	(0.34)	(0.35)	(0.86)	(0.34)	(0.35)
Cont.2	0.880	0.940	0.940	0.888	0.938	0.940	0.928	0.950	0.954
	(0.83)	(0.21)	(0.22)	(0.94)	(0.34)	(0.36)	(0.99)	(0.35)	(0.36)

Table 4: Coverage probabilities and the median length of bootstrapped confidence intervals (in parenthesis) of projection coefficient to linear basis function from M-estimator (M), scaled M-estimator (Sc.M), and mean over 500 repetitions

	Regular			Irregular1			Irregular2		
	Mean	Mt	Sc.M	Mean	M	Sc.Mt	Mean	M	Sc.M
Gaussian	0.940	0.946	0.948	0.940	0.940	0.950	0.944	0.958	0.960
	(0.19)	(0.20)	(0.20)	(0.28)	(0.30)	(0.30)	(0.30)	(0.32)	(0.32)
t(3)	0.928	0.934	0.934	0.946	0.958	0.966	0.940	0.946	0.950
	(0.30)	(0.23)	(0.23)	(0.44)	(0.35)	(0.35)	(0.47)	(0.36)	(0.37)
Cauchy	0.908	0.948	0.942	0.896	0.946	0.95	0.902	0.952	0.940
	(2.06)	(0.29)	(0.31)	(2.56)	(0.46)	(0.51)	(3.23)	(0.48)	(0.54)
Cont.1	0.892	0.940	0.938	0.928	0.956	0.954	0.926	0.942	0.950
	(1.42)	(0.31)	(0.32)	(1.53)	(0.47)	(0.49)	(1.39)	(0.52)	(0.54)
Cont.2	0.918	0.942	0.944	0.888	0.930	0.934	0.936	0.948	0.952
	(1.42)	(0.31)	(0.32)	(1.55)	(0.47)	(0.49)	(1.55)	(0.47)	(0.48)

Table 5: Coverage probabilities and the median length of bootstrapped confidence intervals (in parenthesis) of projection coefficient to constant basis function from M-estimator (M), scaled M-estimator (Sc.M), and mean over 500 repetitions

	Regular			Irregular1			Irregular2		
	Mean	Mt	Sc.M	Mean	M	Sc.Mt	Mean	M	Sc.M
Gaussian	0.950	0.956	0.950	0.944	0.952	0.952	0.954	0.956	0.954
	(0.26)	(0.27)	(0.27)	(0.35)	(0.36)	(0.36)	(0.34)	(0.35)	(0.35)
t(3)	0.908	0.954	0.954	0.916	0.934	0.936	0.940	0.958	0.960
	(0.41)	(0.30)	(0.31)	(0.52)	(0.43)	(0.43)	(0.52)	(0.40)	(0.41)
Cauchy	0.902	0.936	0.934	0.904	0.956	0.960	0.926	0.954	0.952
	(2.92)	(0.38)	(0.42)	(3.04)	(0.55)	(0.61)	(3.51)	(0.51)	(0.57)
Cont.1	0.918	0.964	0.966	0.912	0.950	0.960	0.922	0.948	0.952
	(1.18)	(0.34)	(0.34)	(1.25)	(0.47)	(0.48)	(1.17)	(0.49)	(0.51)
Cont.2	0.918	0.960	0.962	0.874	0.930	0.930	0.914	0.942	0.940
	(1.17)	(0.34)	(0.34)	(1.27)	(0.47)	(0.48)	(1.28)	(0.44)	(0.45)